




Synthesis, DNA-binding, and antitumor activity of polypyridyl-ruthenium(II) complexes [Ru(L)₂(DCIPIP)] (L = bpy, phen; DCIPIP = 2-(2,4-dichlorophenyl)-1*H*-imidazo[4,5-*f*][1,10]phenanthroline)

Shouhai Guan, Tao Pan, Yanyang Zhang, Zhaolin Zeng, Luwen Mu, Duo Zhu, Boyang Chang, Kangdi Zheng, Jiesheng Qian, Qiang Xie, Wenjie Mei, Wenjie Tang & Mingjun Bai

To cite this article: Shouhai Guan, Tao Pan, Yanyang Zhang, Zhaolin Zeng, Luwen Mu, Duo Zhu, Boyang Chang, Kangdi Zheng, Jiesheng Qian, Qiang Xie, Wenjie Mei, Wenjie Tang & Mingjun Bai (2019): Synthesis, DNA-binding, and antitumor activity of polypyridyl-ruthenium(II) complexes [Ru(L)₂(DCIPIP)] (L = bpy, phen; DCIPIP = 2-(2,4-dichlorophenyl)-1*H*-imidazo[4,5-*f*][1,10]phenanthroline), Journal of Coordination Chemistry, DOI: [10.1080/00958972.2019.1630614](https://doi.org/10.1080/00958972.2019.1630614)

To link to this article: <https://doi.org/10.1080/00958972.2019.1630614>

 View supplementary material 

 Published online: 28 Jun 2019.

 Submit your article to this journal 

 View Crossmark data 



Synthesis, DNA-binding, and antitumor activity of polypyridyl-ruthenium(II) complexes [Ru(L)₂(DCIPIP)] (L = bpy, phen; DCIPIP = 2-(2,4-dichlorophenyl)-1*H*-imidazo[4,5-*f*][1, 10]phenanthroline)

Shouhai Guan^a, Tao Pan^a, Yanyang Zhang^a, Zhaolin Zeng^a, Luwen Mu^a, Duo Zhu^a, Boyang Chang^a, Kangdi Zheng^b, Jiesheng Qian^a, Qiang Xie^a, Wenjie Mei^b, Wenjie Tang^a and Mingjun Bai^a

^aDepartment of Vascular Interventional Radiology, The Third Affiliated Hospital, Sun Yat-sen University, Guangzhou, China; ^bSchool of Pharmacy, Guangdong Pharmaceutical University, Guangzhou, China

ABSTRACT

Two new ruthenium(II) complexes, [Ru(bpy)₂(DCIPIP)](ClO₄)₂ (**1**) and [Ru(phen)₂(DCIPIP)](ClO₄)₂ (**2**) (bpy = 2,2'-bipyridine, phen = 1,10-phenanthroline, and DCIPIP = 2-(2,4-dichlorophenyl)-1*H*-imidazo[4,5-*f*][1, 10]phenanthroline), have been prepared in high yield by using microwave-assisted synthesis technology. The anticancer activity of the two ruthenium(II) complexes against A549, C6, CNE-1 and MDA-MB-231 cell lines has been evaluated by MTT assay and results showed that **2** exhibited higher antitumor activity than **1** toward all the selected tumor cell lines. Besides, A549 cell line was sensitive to both ruthenium(II) complexes, especially to **2** (IC₅₀ = 8.01 ± 0.36 μM). Meanwhile, **2** showed low toxicity against MCF-10A human normal cells. Furthermore, the DNA-binding properties of the two new ruthenium(II) complexes with CT-DNA have been investigated by electronic absorption titration, luminescence spectra, circular dichroism spectra and viscosity measurements. The results suggested that **1** and **2** were able to interact with CT-DNA *via* intercalative mode with a strong binding affinity in the order **2** > **1**. All of these results suggested that anticancer activity of both ruthenium(II) complexes could be closely related to their interaction with DNA.

ARTICLE HISTORY

Received 19 October 2018
Accepted 26 May 2019

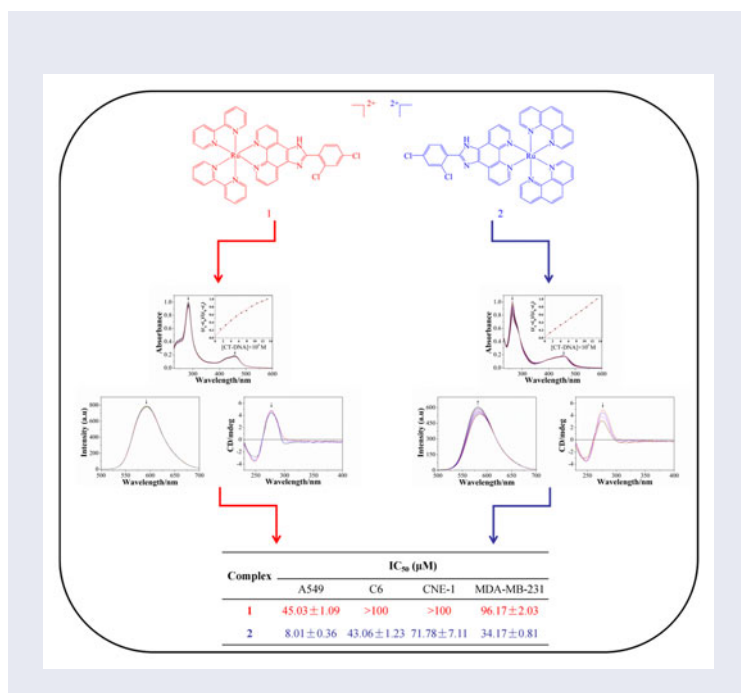
KEYWORDS

Ruthenium(II) polypyridyl complexes; microwave-assisted synthesis; antitumor activity; DNA-binding

CONTACT Wenjie Mei ✉ wenjiemei@126.com; Wenjie Tang ✉ tangwenj@mail.sysu.edu.cn; Mingjun Bai ✉ bzmfxj@163.com

Supplemental data for this article can be accessed [here](#).

© 2019 Informa UK Limited, trading as Taylor & Francis Group



1. Introduction

During the past three decades, the interaction of small molecules with DNA has been studied extensively since DNA is the prime genetic molecule in biological systems and an important cellular target for the discovery of new drugs [1–8]. In general, many antitumor agents exert their anticancer effects through binding to DNA, thereby destroying DNA, blocking DNA-synthesis indirectly and inhibiting cell growth [8–14]. In this respect, ruthenium(II) complexes have gained great attention due to their strong DNA affinity, photochemical properties, high cytotoxicity against cancer cells and low toxicity toward normal cells [15–29]. Previous studies have shown that ruthenium(II) complexes could bind to DNA in three non-covalent binding modes including electrostatic binding, groove-binding and intercalation [30–36]. Ji *et al.* [37] reported that [Ru(bpy)₂(mitatp)](ClO₄)₂ and [Ru(bpy)₂(nitatp)](ClO₄)₂ (mitatp = 5-methoxy-isatino[1,2-b]-1,4,8,9-tetraazatriphenylene; nitatp = 5-nitro-isatino[1,2-b]-1,4,8,9-tetraazatriphenylene) interacted with CT DNA through a typical intercalative mode with a relatively strong affinity and could efficiently photocleave pBR322 DNA under irradiation at UV light ($\lambda = 365$ nm). In recent years, the anticancer activity of ruthenium(II) complexes was extensively investigated [38–41]. Gill *et al.* [42] described that [Ru(dppz)₂(p-HPIP)]²⁺ (dppz = dipyrido[3,2-a:2',3'-c]phenazine, p-HPIP = 2-(4-hydroxyphenyl)imidazo[4,5-f][1,10]phenanthroline) possessed strong DNA-binding affinity and exhibited significant antiproliferative activity against human cervical cancer HeLa cells and human breast cancer MCF-7 cells comparable to that of cisplatin. The results indicated that some ruthenium(II) complexes possessed excellent *in vitro* anticancer activity

against a variety of human tumors cell lines but with low toxicity toward normal cells and *might be considered as potential drug candidates*. In order to obtain more insights into the relationship between antitumor activity of Ru(II) complexes and their interaction with DNA, two new Ru(II) complexes, [Ru(bpy)₂(DCIPIP)](ClO₄)₂ (**1**) and [Ru(phen)₂(DCIPIP)](ClO₄)₂ (**2**) (Scheme 1), were synthesized under microwave irradiation and characterized by elemental analysis, ES-MS, ¹H NMR, and ¹³C NMR. The *in vitro* anticancer activity of **1** and **2** was investigated by 3-(4,5-dimethylthiazol-2-yl)-2,5-diphenyltetrazolium bromide (MTT) method. Their DNA-binding behavior was studied by absorption titration, luminescence spectra, circular dichroism (CD) spectra and viscosity measurements.

2. Experimental

2.1. Chemicals

Ruthenium(III) chloride hydrate, 1,10-phenanthroline-5,6-dione, 2,2'-bipyridine, 1,10-phenanthroline and 2,4-dchlorobenzaldehyde were purchased from Aldrich. Calf-thymus DNA (CT-DNA) was obtained from TaKaRa Biotechnology Co., Ltd. (Dalian, China). Tris-HCl buffer (5 mM Tris-HCl, 50 mM NaCl, pH 7.2) (5 mM Tris-HCl, 50 mM NaCl, pH 7.2) was used for absorption titration, luminescence spectra and CD spectra. *cis*-[Ru(bpy)₂Cl₂] \cdot 2H₂O and *cis*-[Ru(phen)₂Cl₂] \cdot 2H₂O were prepared according to the literature procedures [43, 44].

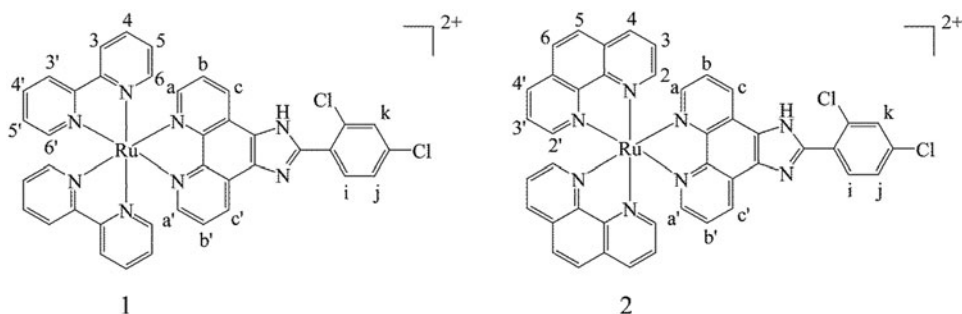
2.2. Instruments

These complexes were synthesized by using an Anton Paar monowave 300 microwave reactor. Electrospray ionization mass spectrometry (ESI-MS) spectra were recorded in acetonitrile on an Agilent 1100 ESI-MS system. ¹H NMR and ¹³C NMR spectra were measured in DMSO-d₆ solution on a Bruker DRX 2500 spectrometer. Electronic absorption spectra were recorded on a Shimadzu UV-2550 spectrophotometer, emission spectra were measured on a Shimadzu RF-5301 fluorescence spectrophotometer, and CD spectra were determined on a Jasco J-810 spectrophotometer.

2.3. Synthesis of complexes

2.3.1. Synthesis of DCIPIP

2-(2,4-Dichlorophenyl)-1*H*-imidazo[4,5-*f*][1,10]phenanthroline (DCIPIP) was prepared according to modified literature procedures which reduced the amount of 2,4-dchlorobenzaldehyde [45, 46]. A mixture of 1,10-phenanthroline-5,6-dione (0.3185 g, 1.5 mmol), 2,4-dichlorobenzaldehyde (0.2652 g, 1.5 mmol), ammonium acetate (4.500 g, 58.4 mmol), and glacial acetic acid (15 mL) was irradiated by microwave for 20 min at 100 °C. Then 50 mL of water was added and the pH value was adjusted to 7.0 at room temperature. A yellow precipitate was filtered and washed with water, dried, and purified by silica gel column (60–100 mesh) using a mixture of C₂H₅OH:CHCl₃ (2:1, v/v) as an eluent. Yield: 85.3%. ESI-MS (C₂H₅OH, m/z): Calcd. for DCIPIP: 365.0 ([M + H]⁺), 731.1 ([2M + H]⁺), 753.0 ([2M + Na]⁺). Found: 365.0 ([M + H]⁺), 730.9 ([2M + H]⁺), 752.9 ([2M + Na]⁺). Anal. Calcd



Scheme 1. The structures of **1** and **2**.

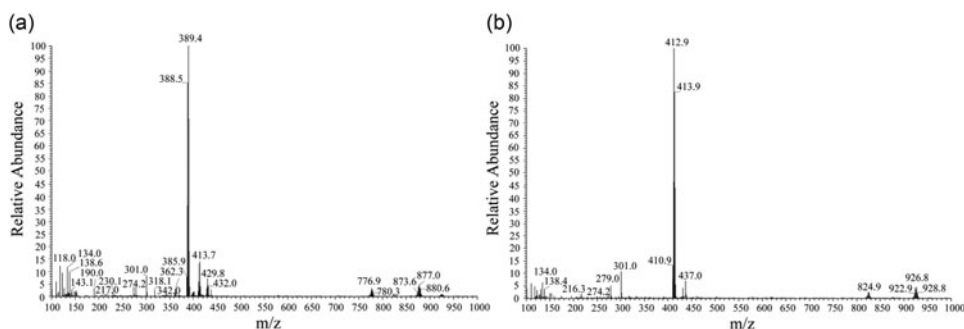


Figure 1. The ESI-MS spectra of (a) **1** and (b) **2**.

for $C_{19}H_{14}Cl_2N_4O_2$ (%): C, 56.87; H, 3.52; N, 13.96. Found (%): C, 57.15; H, 4.00; N, 13.68. IR (KBr, cm^{-1}): 3379 $\nu(N-H)$ 3105 $\nu(C-H)$ and 1607 $\nu(C=N)$. 1H NMR (600 MHz, DMSO- d_6), δ (ppm): 9.07 (d, $J = 2.6$ Hz, 2H), 8.92 (dd, $J = 8.1, 1.7$ Hz, 2H), 8.00 (d, $J = 8.3$ Hz, 1H), 7.92 (d, $J = 2.1$ Hz, 1H), 7.89 – 7.80 (m, 2H), 7.70 (dd, $J = 8.3, 2.1$ Hz, 1H). ^{13}C NMR (151 MHz, DMSO- d_6), δ (ppm): 147.74 (s), 144.15 (s), 135.54 (s), 133.84 (s), 133.47 (s), 130.36 (s), 130.20 (d, $J = 10.4$ Hz), 129.35 (s), 128.25 (s), 126.77 (s).

2.3.2. Synthesis of $[Ru(bpy)_2(DCIPIP)](ClO_4)_2$ (**1**)

$[Ru(bpy)_2(DCIPIP)](ClO_4)_2$ was synthesized by a similar method as the literature [26, 47, 48] with some modifications. A mixture of *cis*- $[Ru(bpy)_2Cl_2] \cdot 2H_2O$ (0.208 mg, 0.4 mmol) and DCIPIP (0.2184 mg, 0.6 mmol) in ethylene glycol (15 mL) was irradiated by microwaves for 25 min at 130 °C. Upon cooling, a red precipitate was obtained by dropwise addition of saturated aqueous $NaClO_4$ solution, then filtered, washed with small amounts of water and diethyl ether, and dried in vacuum. The crude product was dissolved in CH_3CN and purified by column chromatography on neutral alumina using CH_3CN :toluene (2:1, v/v) as an eluant. The second red band was collected and the solvent was evaporated under reduced pressure to afford a red powder. Yield: 82.5%. S_{293K} (H_2O): 0.33 mg/mL. ESI-MS (CH_3CN , m/z): Calcd. for $[Ru(bpy)_2(DCIPIP)](ClO_4)_2$: 389.0 ($[M-2ClO_4]^{2+}$), 777.1 ($[M-2ClO_4-H]^+$), 877.0 ($[M-ClO_4]^+$). Found: 389.4 ($[M-2ClO_4]^{2+}$), 776.9 ($[M-2ClO_4-H]^+$), 877.0 ($[M-ClO_4]^+$) (Figure 1(a)). Anal. Calcd for $C_{41}H_{34}Cl_4N_8O_{10}Ru$ (%): C, 47.28; H, 3.29; N, 10.76. Found (%): C, 47.17; H, 3.46; N, 10.93. IR (KBr, cm^{-1}): 3367 $\nu(N-H)$, 3067 $\nu(C-H)$, 1602 $\nu(C=N)$, 1088 $\nu(ClO_4^-)$ and 625

$\nu(\text{Ru-N})$. ^1H NMR (600 MHz, DMSO-d_6), δ (ppm): 9.05 (dd, $J=8.3, 1.1$ Hz, 2H, H_c, H_c), 8.87 (dd, $J=22.5, 8.2$ Hz, 4H, H_3, H_3), 8.22 (td, $J=8.0, 1.4$ Hz, 2H, H_4), 8.12 (td, $J=8.0, 1.4$ Hz, 2H, H_4), 8.05 (dd, $J=5.2, 0.9$ Hz, 2H, H_a, H_a), 7.98 (d, $J=8.4$ Hz, 1H, H_i), 7.94 (d, $J=2.0$ Hz, 1H, H_k), 7.91 (dd, $J=8.3, 5.3$ Hz, 2H, H_6), 7.88–7.85 (m, 2H, H_b, H_b), 7.71 (dd, $J=8.4, 2.1$ Hz, 1H, H_j), 7.63 (dd, $J=5.6, 0.5$ Hz, 2H, H_6), 7.62–7.58 (m, 2H, H_5), 7.35 (ddd, $J=7.3, 5.7, 1.2$ Hz, 2H, H_5). ^{13}C NMR (151 MHz, DMSO-d_6), δ (ppm): 157.26 (s), 157.03 (s), 151.92 (d, $J=12.7$ Hz), 150.05 (s), 145.50 (s), 138.41 (s), 138.24 (s), 135.64 (s), 133.91 (s), 133.45 (s), 130.84 (s), 130.45 (s), 129.12–127.85 (m), 126.74 (s), 124.87 (d, $J=12.8$ Hz).

2.3.3. Synthesis of $[\text{Ru}(\text{phen})_2(\text{DCIPIP})](\text{ClO}_4)_2$ (2)

$[\text{Ru}(\text{phen})_2(\text{DCIPIP})](\text{ClO}_4)_2$ was obtained in a manner identical to that described for **1**, but using *cis*- $[\text{Ru}(\text{phen})_2(\text{Cl})_2]\cdot 2\text{H}_2\text{O}$ (0.2272 g, 0.4 mmol) in place of *cis*- $[\text{Ru}(\text{bpy})_2\text{Cl}_2]\cdot 2\text{H}_2\text{O}$. Yield: 76.6%. $S_{293\text{K}}$ (H_2O): 0.28 mg/mL. ESI-MS (CH_3CN , m/z): Calcd. for $[\text{Ru}(\text{phen})_2(\text{DCIPIP})](\text{ClO}_4)_2$: 413.0 ($[\text{M}-2\text{ClO}_4]^{2+}$), 825.1 ($[\text{M}-2\text{ClO}_4-\text{H}]^+$), 926.1 ($[\text{M}-\text{ClO}_4]^{2+}$). Found: 412.9 ($[\text{M}-2\text{ClO}_4]^{2+}$), 824.9 ($[\text{M}-2\text{ClO}_4-\text{H}]^+$), 926.8 ($[\text{M}-\text{ClO}_4]^{2+}$) (Figure 1(b)). Anal. Calcd for $\text{C}_{50}\text{H}_{40}\text{Cl}_4\text{N}_8\text{O}_{11}\text{Ru}$ (%): C, 51.25; H, 3.44; N, 9.56. Found (%): C, 51.27; H, 3.65; N, 9.92. IR (KBr, cm^{-1}): 3405 $\nu(\text{N-H})$, 3057 $\nu(\text{C-H})$, 1605 $\nu(\text{C=N})$, 1108 $\nu(\text{ClO}_4^-)$ and 626 $\nu(\text{Ru-N})$. ^1H NMR (600 MHz, DMSO-d_6), δ (ppm): 9.01 (dd, $J=8.3, 1.1$ Hz, 2H, H_c, H_c), 8.78 (dd, $J=5.1, 4.2$ Hz, 4H, H_4, H_4), 8.40 (s, 4H, H_5, H_5), 8.14 (dd, $J=5.3, 1.2$ Hz, 2H, H_2), 8.10 (dd, $J=5.2, 1.2$ Hz, 2H, H_2), 7.99 (dd, $J=10.7, 5.5$ Hz, 2H, H_a, H_a), 7.97 (s, 1H, H_i), 7.91 (d, $J=1.9$ Hz, 1H, H_k), 7.81–7.74 (m, 6H, $\text{H}_3, \text{H}_3, \text{H}_b, \text{H}_b$), 7.72–7.67 (m, 1H, H_j). ^{13}C NMR (151 MHz, DMSO-d_6), δ (ppm): 153.19 (d, $J=20.6$ Hz), 150.25 (s), 147.69 (d, $J=12.3$ Hz), 145.78 (s), 137.23 (d, $J=7.2$ Hz), 135.53–135.01 (m), 133.88 (s), 133.39 (s), 130.92 (s), 130.73 (s), 130.40 (s), 129.39–128.91 (m), 128.53 (d, $J=4.5$ Hz), 128.22 (s), 126.79 (d, $J=6.9$ Hz), 126.48 (s).

2.4. MTT assay

The complexes were tested for anticancer activity using MTT method [49, 50]. Cells were seeded in 96-well microassay culture plates (5×10^3 cells/well) and grown for 24 h at 37°C in a 5% CO_2 incubator. The cells were then incubated in presence of various concentrations of the tested compounds for 72 h at 37°C in a 5% CO_2 incubator. After incubation, 20 μL of the MTT stock solution (5 mg/mL) was added to each well and incubated for 4 h at 37°C . The medium was aspirated from each well and 150 μL /well DMSO was added to solubilize the formazan salt. The absorbance intensity of each well was then measured at 490 nm using a microplate spectrophotometer (MultiskanTM GO, Thermo Scientific, USA).

2.5. DNA-binding properties

2.5.1. Electronic spectra

Absorption spectra titration experiments were performed at room temperature to determine the binding affinity between DNA and complexes. The absorption titrations of the complex in tris-HCl buffer (5 mM Tris-HCl, 50 mM NaCl, pH 7.2) were carried out

by maintaining a constant concentration of the complex (10 μM) to which increments of the DNA stock solution were added. The titration processes were repeated several times until the spectra did not change, indicating that binding saturation has been achieved. The intrinsic binding constants for the complexes with CT-DNA (K_b) were obtained by monitoring the changes in absorbance of the metal-to-ligand charge-transfer (MLCT) band with increasing concentration of DNA using the following equation [51, 52]:

$$(\varepsilon_a - \varepsilon_f) / (\varepsilon_b - \varepsilon_f) = \left[b - (b^2 - 2K_b^2 C_t [\text{DNA}] / s) \right]^{1/2} / 2K_b C_t \quad (1a)$$

$$b = 1 + K_b C_t + K_b [\text{DNA}] / 2s \quad (1b)$$

where [DNA] is the concentration of CT-DNA in the base pair, ε_a , ε_f , and ε_b correspond to the apparent absorption coefficient ($A_{\text{obsd}}/[\text{complex}]$) observed for the MLCT absorption band at the given DNA concentration, the extinction coefficient of the free complex in the solution, and the extinction coefficient of the complex in fully bound form, respectively. K_b is the equilibrium binding constant (M^{-1}), C_t is the total metal complex concentration in nucleotides and s is the binding site size.

2.5.2. Fluorescence emission titrations

The binding interaction of the complexes with DNA was also investigated using fluorescence spectroscopy. Fluorescence experiments in tris-HCl buffer (5 mM Tris-HCl, 50 mM NaCl, pH 7.2) were performed using a fixed complex concentration (10 μM), and at the same time gradually increasing CT-DNA concentration. Before the measurements, the mixture was shaken and incubated at room temperature for 5 min. The samples were excited at 340 nm and the *emission* spectra were collected in the range of 500–700 nm.

2.5.3. CD measurements

The CD spectra were measured on a Jasco J-810 CD spectrometer at 37 $^\circ\text{C}$ in the wavelength range of 230–400 nm. The CD titration experiment in tris-HCl buffer (5 mM Tris-HCl, 50 mM NaCl, pH 7.2) was performed at a fixed CT-DNA concentration (100 μM) with various concentrations of the complexes. The reaction was stirred thoroughly and allowed to equilibrate for 5 min until no elliptical changes were observed before data collection.

2.5.4. Viscosity measurements

The viscosity measurement is an effective method to authenticate the binding mode of the compounds with CT-DNA [53]. Viscosity studies were taken using an Ubbelohde viscometer in a thermostatic bath maintained at 30.0 ± 0.1 $^\circ\text{C}$. During the measurement, fixed solutions of complexes and DNA in different concentrations were prepared in Tris-HCl buffer medium. Data were presented as $(\eta/\eta_0)^{1/3}$ versus binding ratio ($R = [\text{Ru}]/[\text{DNA}] = 0.0\text{--}1.6$), where η and η_0 is the viscosity of DNA in the presence and absence of complexes, respectively [54]. Relative viscosities for CT-DNA in the presence and absence of complexes were calculated from the relation $\eta = (t - t_0)/t_0$, where t is the flow time of DNA containing solution and t_0 is the flow time of Tris-HCl buffer alone.

3. Results and discussion

3.1. Synthesis and characterization

Compared with the traditional thermal heating method, the microwave-assisted synthesis heating technology can effectively reduce the reaction time and significantly improve the yield of the compound [55, 56]. Herein, **1** and **2** with high efficiency were synthesized by microwave-assisted synthesis technology [26]. The temperature of reaction system rapidly reached 130 °C in 1 min under microwave irradiation, after then, it remained almost unchanged during the whole reaction process (Figure S1). The yields of **1** and **2** under the irradiation of microwave were about 82.5% and 76.6%, respectively. Complexes **1** and **2** were confirmed by electrospray mass spectrometry (ES-MS), ^1H NMR and ^{13}C NMR spectra.

The chemical shifts in the ^1H NMR spectra of **1** were attributed to the protons of $\text{H}_{4'}$, H_4 , $\text{H}_{6'}$ and H_6 in each bipyridyl ligand that appeared at 8.22, 8.12, 7.91 and 7.63 ppm, respectively (Figure 2(a)). The peaks at 8.87, 7.62–7.58 and 7.35 ppm were ascribed to $\text{H}_{3'}$ and H_3 , $\text{H}_{5'}$, H_5 in each bipyridyl ligand, respectively. Moreover, the chemical shifts were attributed to $\text{H}_{a'}$ and H_a , $\text{H}_{b'}$ and H_b , $\text{H}_{c'}$ and H_c in the phenanthroline ring appeared at 8.05, 7.88–7.85 and 9.05 ppm, respectively. Besides, the chemical shifts at 7.98, 7.71 and 7.94 ppm could be ascribed to H_i , H_j and H_k in the benzene group, respectively. For **2**, a characteristic chemical shift attributed to H_5 and H_6 in co-ligand phenanthroline appeared at 8.40 ppm (Figure 2(b)).

Hydrolysis studies of **1** and **2** were carried out in tris-HCl buffer (5 mM Tris-HCl, 50 mM NaCl, pH 7.2) using both ES-MS and UV-vis spectroscopy to monitor the changes. There were no observable changes in the spectra of **1** and **2** over 5 days (Figures S2 and S3), indicating that **1** and **2** were stable in tris-HCl buffer (5 mM Tris-HCl, 50 mM NaCl, pH 7.2).

3.2. Anticancer activity studies

The *in vitro* antitumor activities of **1** and **2** against human lung adenocarcinoma cells (A549), rat glioma cells (C6), human nasopharyngeal carcinoma cells (CNE-1), and human breast cancer cells (MDA-MB-231) were evaluated by MTT assay after 72-h treatment. The IC_{50} values obtained of **1** and **2** against the selected four cancer cell lines are shown in Table 1. Comparing the IC_{50} values of both ruthenium(II) complexes,

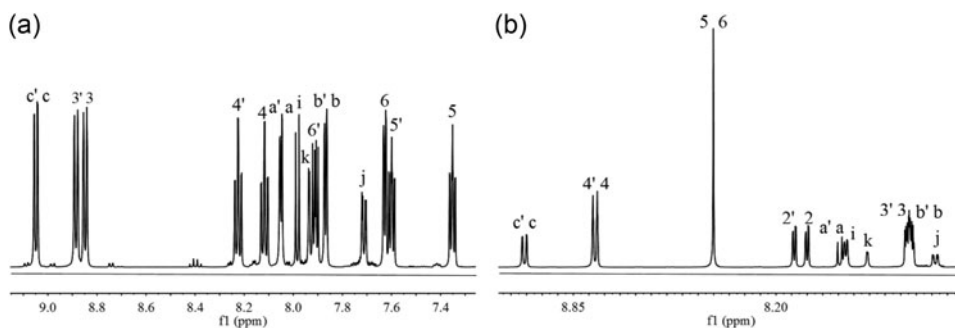


Figure 2. The ^1H NMR spectra of (a) **1** and (b) **2**.

Table 1. The IC₅₀ values of **1** and **2** against the selected cell lines and the corresponding lipophilicity (*P*).

Complex	IC ₅₀ (μM)					log <i>P</i>
	A549	C6	CNE-1	MDA-MB-231	MCF-10A	
1	45.03 ± 1.09	>100	>100	96.17 ± 2.03	>100	-1.27
2	8.01 ± 0.36	43.06 ± 1.23	71.78 ± 7.11	34.17 ± 0.81	>100	-0.53

2 showed *higher anticancer activity* than **1** against all the selected tumor cell lines under the same conditions. Moreover, both complexes exhibited acceptable antiproliferative activity against A549 cells, especially **2** (IC₅₀ = 8.01 ± 0.36 μM), but with low toxicity toward normal human mammary epithelial cells (MCF-10A). The lipophilicity of an anticancer agent has a vital influence on its cytotoxicity. It has been reported that the cytotoxic activities of Ru(II) complexes are positively correlated with their lipophilicities, probably because a higher lipophilicity influences the cellular uptake and cytotoxicity of phen derivatives [57]. The possible reason causing the different antitumor activities for both Ru(II) complexes is that the ancillary phen is more hydrophobic than bpy. Thus, we investigated the lipophilicity partition coefficient. The lipophilicity partition coefficients for **1** and **2** were approximately -1.27 and -0.53, respectively (Table 1). The hydrophobicity of phenanthroline confers stronger lipophilicity to **2**, which may result in higher anticancer activity of **2** than **1**. In addition, comparing the IC₅₀ values of both complexes against A549 cells with other Ru(II) complexes: [Ru(phen)₂(mitatp)]²⁺ (20 μM) [58], [Ru(bpy)₂(mitatp)]²⁺ (52 μM) [58], [Ru(phen)₂(PIP)]²⁺ (>100 μM) [59] and [Ru(phen)₂(*p*-TFPIP)]²⁺ (43.4 ± 5.3 μM) [59], **1** and **2** showed high cytotoxic activity. These results were reasonable given that the introduction of electron-withdrawing substituent (Cl in DCIPIP) to the end benzene ring of phenanthroimidazole ligand may enhance the biological activity of its Ru(II) complexes [60]. The results obtained suggested that **2** showed promising inhibitory activity against a variety of tumors cells, particularly for A549 cell line.

3.3. DNA-binding studies

DNA is considered to be a potential intracellular target of many Ru(II) complexes that inhibit the growth of cancer cells [61]. DNA binding is the critical step in the process of DNA cleavage in most cases and has importance in understanding the potential antitumor mechanism [62]. Therefore, it is indeed to investigate the interaction of both complexes with CT-DNA. The experiments were carried out by electronic absorption titration, luminescence spectra, circular dichroic spectra, and viscosity measurements.

3.3.1. Electronic absorption titration

The application of electronic absorption spectroscopy in DNA-binding studies is the most common method for probing the interaction between metal complexes with DNA [63, 64]. In general, the absorption spectra of metal complexes exhibited different extents of hypochromism and red-shift in the presence of DNA, and the degree of change depends on the binding affinity [65, 66]. The electronic absorption spectra of **1** and **2** in the presence of increasing amounts of CT-DNA are given in Figure 3.

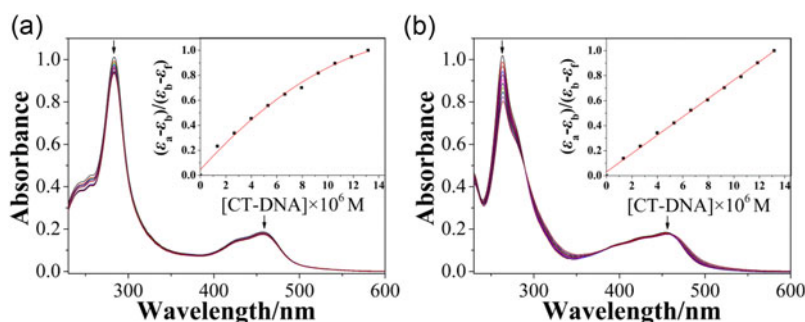


Figure 3. Electronic absorption spectra of (a) **1** and (b) **2** in tris-HCl buffer (5 mM Tris-HCl, 50 mM NaCl, pH 7.2) upon addition of CT-DNA. [Complex] = 10 μ M, [DNA] = 1 mM. The arrows indicate the absorption intensity change upon increase of CT-DNA concentration.

As shown in **Figure 3**, the electronic spectra of **1** and **2** in tris-HCl buffer (5 mM Tris-HCl, 50 mM NaCl, pH 7.2) showed the characteristic intra-ligand (IL) transitions at 250–300 nm assigned to the internal π - π^* transition of the ligand and the typical metal-to-ligand charge transfer (MLCT) absorption bands in the 350–500 nm region attributed to the overlap of Ru(d π) \rightarrow bpy or phen (π^*) and Ru(d π) \rightarrow DCIPIP (π^*). The characteristic IL absorption band appeared at 283.5 and 263.5 nm for **1** and **2**, respectively. The lowest-energy bands at 457.5 nm for **1** and 453 nm for **2** were assigned to the MLCT transition. In addition, the measured molar extinction coefficients (ϵ) of the low-energy MLCT absorption bands at 457.5 nm of **1** and 453.0 nm of **2** were 1.87×10^4 and 1.85×10^4 M $^{-1}$ cm $^{-1}$, respectively.

Complex-binding to DNA in the intercalation mode usually results in hypochromism and bathochromism in the absorption spectra, due to a strong π - π stacking interaction between an aromatic chromophore and the base pairs of DNA. Upon addition of CT-DNA, the IL and MLCT transitions of **1** exhibited hypochromism of about 8 and 5%, and those of **2** were observed approximately 21% and 4% hypochromism at the same conditions, respectively. The intrinsic binding constant K_b of **1** and **2** were also determined by monitoring the changes in absorbance at the MLCT bands with increasing concentration of CT-DNA, giving K_b of 4.56×10^5 and 5.57×10^5 M $^{-1}$, respectively. The K_b values obtained for **1** (4.56×10^5 M $^{-1}$) and **2** (5.57×10^5 M $^{-1}$) were much higher than those for claimed DNA intercalators of [Ru(bpy) $_2$ (DPT)] $^{2+}$ (2.1×10^4 M $^{-1}$) [67], [Ru(bpy) $_2$ (TATP)] $^{2+}$ (6.3×10^4 M $^{-1}$) [67], [Ru(dmp) $_2$ (DNPIP)] $^{2+}$ (6.24×10^4 M $^{-1}$) [68], and [Ru(dmp) $_2$ (DAPIP)] $^{2+}$ (1.64×10^4 M $^{-1}$) [68]. Then, these results indicated that both complexes bound to double-stranded DNA *via* intercalating mode and **2** (5.57×10^5 M $^{-1}$) exhibited a stronger DNA-binding affinity than **1** (4.56×10^5 M $^{-1}$), which may lead to **2** having higher antitumor activity than **1**.

The DNA-binding constant K_b of **2** (5.57×10^5 M $^{-1}$) was higher than that of **1** (4.56×10^5 M $^{-1}$), which may be due to the ancillary ligand. On going from bpy to phen, the plane area and hydrophobicity increase, leading to a higher binding affinity to DNA for **2** [69]. These values were smaller than those of classical intercalators, such as [Ru(bpy) $_2$ (dppz)] $^{2+}$ (4.9×10^6 M $^{-1}$) [70] and [Ru(bpy) $_2$ (ppd)] $^{2+}$ (1.3×10^6 M $^{-1}$) [71], but comparable to that of [Ru(phen) $_2$ (7-NO $_2$ -dppz)] $^{2+}$ (3.56×10^5 M $^{-1}$) [72], [Ru(phen) $_2$ (7-F-dppz)] $^{2+}$ (5.41×10^5 M $^{-1}$) [73], [Ru(bpy) $_2$ (pip)] $^{2+}$ (4.70×10^5 M $^{-1}$) [74],

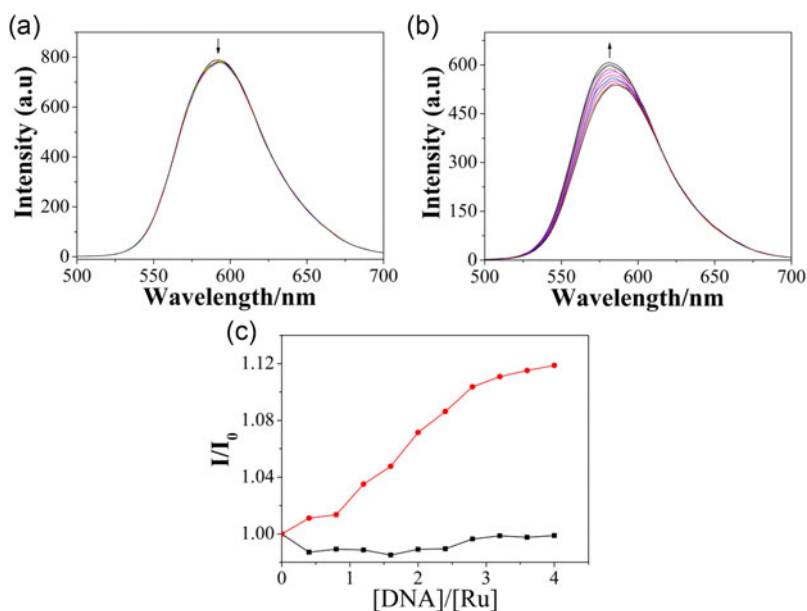


Figure 4. Emission spectra of (a) **1** and (b) **2** in tris-HCl buffer (5 mM Tris-HCl, 50 mM NaCl, pH 7.2) in the absence and presence of CT-DNA. [Complex] = 10 μ M, [DNA] = 1 mM. Arrow refers to the emission intensity change upon increasing CT-DNA concentrations. (c) The changes of emission of **1** (■) and **2** (●) in increasing amounts of CT-DNA.

and $[\text{Ru}(\text{phen})_2(\text{dppca})]^{2+}$ ($3.4 \times 10^5 \text{ M}^{-1}$) [75], which suggested that **1** and **2** exhibited certain affinities to double-helical DNA. Moreover, the binding constants of **1** and **2** were higher than those of $[\text{Ru}(\text{phen})_2(o\text{-MPIP})]^{2+}$ ($0.35 \times 10^5 \text{ M}^{-1}$) [76], $\Delta\text{-}[\text{Ru}(\text{bpy})_2(p\text{-HPIP})]^{2+}$ ($1.0 \times 10^5 \text{ M}^{-1}$) [43], $\Lambda\text{-}[\text{Ru}(\text{bpy})_2(p\text{-HPIP})]^{2+}$ ($0.7 \times 10^5 \text{ M}^{-1}$) [43], $[\text{Ru}(\text{bpy})_2(\text{BTCP})]$ ($5.52 \times 10^4 \text{ M}^{-1}$) [77], and $\text{Ru}(\text{phen})_2(\text{BTCP})]$ ($8.80 \times 10^4 \text{ M}^{-1}$) [77] because of the presence of electron-withdrawing substituent (Cl in DCIPIP) on the intercalative ligand which increased the DNA-binding affinity [78, 79].

3.3.2. Fluorescence emission titrations

Fluorescence emission spectra of **1** and **2** were also used to clarify the nature of the interaction between the complexes and double helix CT-DNA, and the results are shown in Figure 4. In the absence of CT-DNA, **1** and **2** could emit strong luminescence in tris-HCl buffer (5 mM Tris-HCl, 50 mM NaCl, pH 7.2) in the range 500–700 nm at room temperature, with maxima appearing at 595 and 586 nm, respectively. The quantum yields of **1** and **2** in CH_3CN were 0.075 and 0.101, respectively. In addition, the excited state lifetimes for **1** and **2** were determined to be 415 and 530 ns, respectively.

Upon addition of DNA, the luminescence intensity of **2** presented a remarkable increase (Figure 4(b)), but that of **1** showed only a *small change* (Figure 4(a)). When the ratio of $[\text{DNA}]/[\text{complex}]$ of 4:1 for **2** reached a saturating value, the emission intensity of **2** increased to about 1.12 times larger than the original, implying that **2** could interact with CT-DNA (Figure 4(c)). The enhancement of emission intensities of **2** could be attributed to the hydrophobic environment inside the DNA helix, which protected **2** from being quenched by water molecules. In addition, the fluorescence

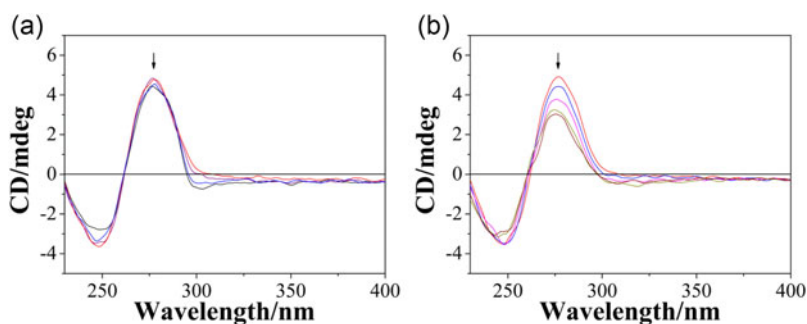


Figure 5. Circular dichroic spectra of CT-DNA in tris-HCl buffer (5 mM Tris-HCl, 50 mM NaCl, pH 7.2) in the absence and presence of increasing amounts of (a) **1** and (b) **2**. [DNA] = 100 μ M, [Complex] = 0–8 μ M. Arrow indicates the absorbance change upon increasing amounts of complexes.

intensity of **1** decreased slightly with the increased DNA concentration, however, this was not a significant observation and could be attributed to a dilution effect due to the incrementally added DNA volume, which indicated that **1** exhibited weak interaction with duplex strand DNA. These data were in agreement with that of electronic absorption spectroscopy, indicating that **2** bound to DNA more strongly than **1**.

3.3.3. CD studies

CD spectroscopy is an extremely useful technique to study conformational change of biology molecules, so it is widely used to study the interaction of small molecules with DNA [64]. The CD spectra of CT-DNA in the absence and presence of **1** and **2** are shown in Figure 5. In the absence of complexes, the CD spectra of CT-DNA in tris-HCl buffer (5 mM Tris-HCl, 50 mM NaCl, pH 7.2) exhibited two characteristic CD signals with a positive peak at about 277 nm and a negative peak at about 247 nm. Upon increasing the concentration of **2**, the positive CD signal of CT-DNA decreased distinctly, indicating that the conformation of CT-DNA was disturbed by **2** and there was strong interaction between **2** and CT-DNA. However, minor changes in the CD spectra were observed in the presence of **1**, suggesting that **1** did not display significant effect on the conformation of CT-DNA. Therefore, the CD results indicated that **2** bound more strongly to CT-DNA than **1**. These data were also consistent with the above studies, indicating that the DNA-binding property can be closely related to the antitumor activity of the complexes.

3.3.4. Viscosity studies

In order to clarify the binding modes of **1** and **2** with CT-DNA, viscosity measurements which are sensitive to the length change of CT-DNA were performed [80]. It is well-known that a classical intercalation model generally results in lengthening of the DNA helix, as DNA-base pairs are separated to accommodate the binding compound, leading to a significant increase in viscosity of DNA solution. In contrast, a partial and/or non-classic (like external groove-binding or electrostatic interaction) intercalation of the complex causes a bend or kink in the DNA-helix, reducing its effective length; in such cases, the changes in DNA viscosity is decreased or there is no change at all [81].

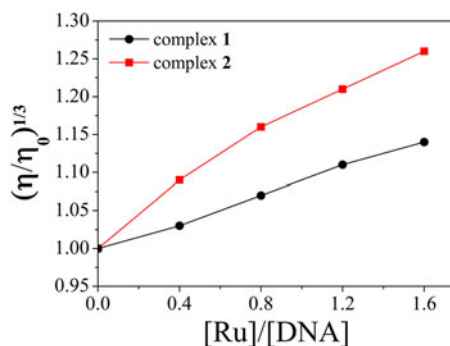


Figure 6. Effect of increasing amounts of (a) **1** (●) and (b) **2** (■) on the relative viscosity of calf-thymus DNA at 30 ± 0.1 °C. [DNA] = 0.25 mM.

The effects of **1** and **2** on the relative viscosity of CT-DNA are shown in Figure 6. Upon increasing concentration of **1** and **2**, the relative viscosity of CT-DNA solution increased steadily. The increased degree of viscosity, which may depend on its affinity to DNA, follows the order of $2 > 1$. The results indicated that **1** and **2** interact with CT-DNA *via* intercalative mode and correspond to electronic absorption titration results above.

4. Conclusion

Two new ruthenium(II) complexes, $[\text{Ru}(\text{bpy})_2(\text{DCIPIP})](\text{ClO}_4)_2$ (**1**) and $[\text{Ru}(\text{phen})_2(\text{DCIPIP})](\text{ClO}_4)_2$ (**2**), have been synthesized in high yield under irradiation of microwave, and characterized by elemental analysis, ESI-MS, ^1H NMR and ^{13}C NMR spectroscopy. According to MTT results, **2** exhibited higher antitumor activity than **1** against A549, C6, CNE-1 and MDA-MB-231 cell lines. Notably, A549 cell line was susceptible to both complexes, especially to **2**. Furthermore, the DNA-binding behavior of the complexes was investigated by electronic absorption titration, luminescence spectra, CD spectra and viscosity measurements. The results indicated that **1** and **2** interact with CT-DNA through intercalative mode. Moreover, **2** binds to DNA more strongly than **1**, which is consistent with the antitumor activity. Taken together, these results demonstrated that both complexes, especially **2**, might exhibit an inhibitory effect on the proliferation of tumor cells through binding to DNA.

Disclosure statement

Shouhai Guan and Tao Pan contributed equally to the work. No potential conflict of interest was reported by the authors.

Funding

This work was supported by the National Nature Science Foundation of China [grant number 81572926, 81703349]; the Provincial Major Scientific Research Projects in Universities of Guangdong Province [grant number 2014KZDXM053]; the Science and Technology Project of Guangdong Province [grant number 2014A020212312, 2017zc0213]; the Innovation Projects in Universities of Guangdong Province [grant number 2015cxqx151]; the Tradition Chinese

Medicine Bureau of Guangdong Province [grant number 20151265]; the Innovation Team Projects in Universities of Guangdong Province [grant number 2016KCXTD018]; the Major Project of the Education Department of Guangdong Province [grant number 2017KZDXM051]; and the Technology Plan of Guangdong Province-Social Development Project [grant number 2017A020215021].

References

- [1] J.K. Barton. *Science*, **233**, 727 (1986).
- [2] B.A. Jackson, V.Y. Alekseyev, J.K. Barton. *Biochemistry*, **38**, 4655 (1999).
- [3] G. Psomas, A. Tarushi, E.K. Efthimiadou. *Polyhedron*, **27**, 133 (2008).
- [4] L.N. Ji, X.H. Zou, J.G. Liu. *Coord. Chem. Rev.*, 216-217, 513 (2001).
- [5] Y.T. Sun, S.Y. Bi, D.Q. Song, C.Y. Qiao, D. Mu, H.Q. Zhang. *Sens. Actuators B*, **129**, 799 (2008).
- [6] C.V. Kumar, R.S. Turner, E.H. Asuncion. *J. Photochem. Photobiol. A*, **74**, 231 (1993).
- [7] K.C. Skyrianou, C.P. Raptopoulou, V. Psycharis, D.P. Kessissoglou, G. Psomas. *Polyhedron*, **28**, 3265 (2009).
- [8] J. Kljun, I. Bratsos, E. Alessio, G. Psomas, U. Repnik, M. Butinar, B. Turk, I. Turel. *Inorg. Chem.*, **52**, 9039 (2013).
- [9] G.R. Fulmer, A.J.M. Miller, N.H. Sherden, H.E. Gottlieb, A. Nudelman, B.M. Stoltz, J.E. Bercaw, K.I. Goldberg. *Organometallics*, **29**, 2176 (2010).
- [10] K.J. Du, J.Q. Wang, J.F. Kou, G.Y. Li, L.L. Wang, H. Chao, L.N. Ji. *Eur. J. Med. Chem.*, **46**, 1056 (2011).
- [11] X.Y. Wang, Z.J. Guo. *Chem. Soc. Rev.*, **42**, 202 (2013).
- [12] Y.H. Li, B.D. Wang, Z.Y. Yang. *Spectrochim Acta A Mol Biomol Spectrosc*, **67**, 395 (2007).
- [13] K.S. Lovejoy, S.J. Lippard. *Dalton Trans.*, **48**, 10651 (2009).
- [14] A. Bergamo, G. Sava. *Dalton Trans.*, **40**, 7817 (2011).
- [15] F. Gao, H. Chao, F. Zhou, X. Chen, Y.F. Wei, L.N. Ji. *J. Inorg. Biochem.*, **102**, 1050 (2008).
- [16] C.S. Devi, D.A. Kumar, S.S. Singh, N. Gabra, N. Deepika, Y.P. Kumar, S. Satyanarayana. *Eur. J. Med. Chem.*, **64**, 410 (2013).
- [17] A.K. Gorle, A.J. Ammit, L. Wallace, F.R. Keene, J.G. Collins. *New J. Chem.*, **38**, 4049 (2014).
- [18] G. Sava, S. Pacor, A. Bergamo, M. Cocchietto, G. Mestroni, E. Alessio. *Chem. Biol. Interact.*, **95**, 109 (1995).
- [19] A. Tadić, J. Poljarević, M. Krstić, M. Kajzerberger, S. Arandelović, S. Radulović, C. Kakoulidou, A.N. Papadopoulos, G. Psomas, S. Grgurić-Sipka. *New J. Chem.*, **42**, 3001 (2018).
- [20] A. Levina, A. Mitra, P.A. Lay. *Metallomics*, **1**, 458 (2009).
- [21] G. Süß-Fink. *Dalton Trans.*, **39**, 1673 (2010).
- [22] G. Gasser, I. Ott, N. Metzler-Nolte. *J. Med. Chem.*, **54**, 3 (2011).
- [23] S. Thota, S. Vallala, M. Imran, S. Mekala, S.S. Anchuri, S.S. Karki, R. Yerra, J. Balzarini, E.D. Clercq. *J. Coord. Chem.*, **66**, 1031 (2013).
- [24] W.A. Wani, Z. Al-Othman, I. Ali, K. Saleem, M.F. Hsieh. *J. Coord. Chem.*, **67**, 2110 (2014).
- [25] G.L. Ma, X.D. Bi, F. Gao, Z. Feng, D.C. Zhao, F.J. Lin, R. Yan, D.D. Liu, P. Liu, J.B. Chen, H.B. Zhang. *J. Inorg. Biochem.*, **185**, 1 (2018).
- [26] Z. Zhang, Q. Wu, X.H. Wu, F.Y. Sun, L.M. Chen, J.C. Chen, S.L. Yang, W.J. Mei. *Eur. J. Med. Chem.*, **80**, 316 (2014).
- [27] Q. Wu, J.T. He, W.J. Mei, Z. Zhang, X.H. Wu, F.Y. Sun. *Metallomics*, **6**, 2204 (2014).
- [28] Q. Wu, K.D. Zheng, S.Y. Liao, Y. Ding, Y.Q. Li, W.J. Mei. *Organometallics*, **35**, 317 (2016).
- [29] L. Perdisatt, S. Moqadasi, L. O'Neill, G. Hessman, A. Ghion, M.Q.M. Warraich, A. Casey, C. O'Connor. *J. Inorg. Biochem.*, **182**, 71 (2018).
- [30] H. Song, J.T. Kaiser, J.K. Barton. *Nat. Chem.*, **4**, 615 (2012).
- [31] J.G. Liu, B.H. Ye, H. Li, L.N. Ji, R.H. Li, J.Y. Zhou. *J. Inorg. Biochem.*, **73**, 117 (1999).

- [32] R. Gaur, L. Mishra. *Inorg. Chem.*, **51**, 3059 (2012).
- [33] H. Niyazi, J.P. Hall, K. O'Sullivan, G. Winter, T. Sorensen, J.M. Kelly, C.J. Cardin. *Nat. Chem.*, **4**, 621 (2012).
- [34] C.J. Cardin, J.M. Kelly, S.J. Quinn. *Chem. Sci.*, **8**, 4705 (2017).
- [35] J.P. Hall, P.M. Keane, H. Beer, K. Buchner, G. Winter, T.L. Sorensen, D.J. Cardin, J.A. Brazier, C.J. Cardin. *Nucleic Acids Res.*, **44**, 9472 (2016).
- [36] N.M. Gabra, B. Mustafa, Y.P. Kumar, C.S. Devi, A. Srishailam, P.V. Reddy, K.L. Reddy, S. Satyanarayana. *J. Fluoresc.*, **24**, 169 (2014).
- [37] H.J. Yu, S.M. Huang, L.Y. Li, H.N. Jia, H. Chao, Z.W. Mao, J.Z. Liu, L.N. Ji. *J. Inorg. Biochem.*, **103**, 881 (2009).
- [38] J.Q. Cao, Q. Wu, W.J. Zheng, L. Li, W.J. Mei. *RSC Adv.*, **7**, 26625 (2017).
- [39] J.Q. Wang, J.F. Kou, Z.Z. Zhao, K.Q. Qiu, H. Chao. *Inorg. Chem. Front.*, **4**, 1003 (2017).
- [40] B. Purushothaman, P. Arumugam, H. Ju, G. Kulsli, A.A.S. Samson, J.M. Song. *Eur. J. Med. Chem.*, **156**, 747 (2018).
- [41] A.F. Tikum, Y.J. Jeon, J.H. Lee, M.H. Park, I.Y. Bae, S.H. Kim, H.J. Lee, J. Kim. *J. Inorg. Biochem.*, **180**, 204 (2018).
- [42] M.R. Gill, S.N. Harun, S. Halder, R.A. Boghozian, K. Ramadan, H. Ahmad, K.A. Vallis. *Sci. Rep.*, **6**, 31973 (2016).
- [43] W.J. Mei, J. Liu, K.C. Zheng, L.J. Lin, H. Chao, A.X. Li, F.C. Yun, L.N. Ji. *Dalton Trans.*, **7**, 1352 (2003).
- [44] B.P. Sullivan, D.J. Salmon, T.J. Meyer. *Inorg. Chem.*, **17**, 3334 (1978).
- [45] K.A. Kumar, K.L. Reddy, S. Satyanarayana. *J. Coord. Chem.*, **63**, 3676 (2010).
- [46] S.Y. Liao, Z. Zhang, Q. Wu, X.C. Wang, W.J. Mei. *Bioorg. Med. Chem.*, **22**, 6503 (2014).
- [47] F. Hayat, Zia-ur-Rehman, M.H. Khan. *J. Coord. Chem.*, **70**, 279 (2017).
- [48] H. Chao, R.H. Li, C.W. Jiang, H. Li, L.N. Ji, X.Y. Li. *J. Chem. Soc., Dalton Trans.*, **12**, 1920 (2001).
- [49] N.D. McClenaghan, Y. Leydet, B. Maubert, M.T. Indelli, S. Campagna. *Coord. Chem. Rev.*, **249**, 1336 (2005).
- [50] T. Mosmann. *J. Immunol. Methods*, **65**, 55 (1983).
- [51] L.M. Chen, J. Liu, J.C. Chen, C.P. Tan, S. Shi, K.C. Zheng, L.N. Ji. *J. Inorg. Biochem.*, **102**, 330 (2008).
- [52] R.B. Nair, E.S. Teng, S.L. Kirkland, C.J. Murphy. *Inorg. Chem.*, **37**, 139 (1998).
- [53] G.N. Yu, J.C. Huang, L. Li, R.T. Liu, J.Q. Cao, Q. Wu, S.Y. Zhang, C.X. Wang, W.J. Mei, W.J. Zheng. *RSC Adv.*, **8**, 30573 (2018).
- [54] G. Cohen, H. Eisenberg. *Biopolymers*, **8**, 45 (1969).
- [55] F.A. Beckford, J. Michael Shaloski, G. Leblanc, J. Thessing, L.C. Lewis-Alleyne, A.A. Holder, L. Li, N.P. Seeram. *Dalton Trans.*, **48**, 10757 (2009).
- [56] Q. Wu, J. Wu, W.J. Mei, Q. Wang, Z. Zhang, X.H. Wu, F.Y. Sun, W.L. Wu, Y.H. Chen, X.Y. Hu. *Aust. J. Chem.*, **66**, 1422 (2013).
- [57] C.P. Tan, S.H. Wu, S.S. Lai, M.X. Wang, Y. Chen, L.J. Zhou, Y.P. Zhu, W. Lian, W.L. Peng, L.N. Ji, A.L. Xu. *Dalton Trans.*, **40**, 8611 (2011).
- [58] H.J. Yu, Y. Chen, L. Yu, Z.F. Hao, L.H. Zhou. *Eur. J. Med. Chem.*, **55**, 146 (2012).
- [59] L.L. Zeng, Y. Chen, J.P. Liu, H.Y. Huang, R.L. Guan, L.N. Ji, H. Chao. *Sci. Rep.*, **6**, 1949 (2016).
- [60] Y.M. Li, Q. Wu, G.N. Yu, L. Li, X.Y. Zhao, X.T. Huang, W.J. Mei. *Eur. J. Med. Chem.*, **164**, 282 (2019).
- [61] E. Gallori, C. Vettori, E. Alessio, F.G. Vilchez, R. Vilaplana, P. Orioli, A. Casini, L. Messori. *Arch. Biochem. Biophys.*, **376**, 156 (2000).
- [62] R. Nomula, X.Y. Wu, J.Z. Zhao, N.R. Munirathnam. *Mater. Sci. Eng. C Mater. Biol. Appl.*, **79**, 710 (2017).
- [63] J.K. Barton, A. Danishefsky, J. Goldberg. *J. Am. Chem. Soc.*, **106**, 2172 (1984).
- [64] J. Sun, S. Wu, H.Y. Chen, F. Gao, J. Liu, L.N. Ji, Z.W. Mao. *Polyhedron*, **30**, 1953 (2011).
- [65] A.M. Pyle, J.P. Rehmann, R. Meshoyrer, C.V. Kumar, N.J. Turro, J.K. Barton. *J. Am. Chem. Soc.*, **111**, 3051 (1989).
- [66] L. Tan, J. Shen, J. Liu, L. Zeng, L. Jin, C. Weng. *Dalton Trans.*, **41**, 4575 (2012).

- [67] H. Deng, J.W. Cai, H. Xu, H. Zhang, L.N. Ji. *Dalton Trans.*, **3**, 325 (2003).
- [68] Z.Z. Li, Z.H. Liang, H.L. Huang, Y.J. Liu. *J. Mol. Struct.*, **1001**, 36 (2011).
- [69] H. Xu, K.C. Zheng, H. Deng, L.J. Lin, Q.L. Zhang, L.N. Ji. *New J. Chem.*, **27**, 1255 (2003).
- [70] A.E. Friedman, J.C. Chambron, J.P. Sauvage, N.J. Turro, J.K. Barton. *J. Am. Chem. Soc.*, **112**, 4960 (1990).
- [71] F. Gao, H. Chao, F. Zhou, Y.X. Yuan, B. Peng, L.N. Ji. *J. Inorg. Biochem.*, **100**, 1487 (2006).
- [72] K.L. Reddy, Y. H.K. Reddy, S. Satyanarayana. *Nucleos. Nucleot. Nucleic Acids* **28**:10, 953 (2009).
- [73] N. Deepika, Y.P. Kumar, C.S. Devi, P.V. Reddy, A. Srishailam, S. Satyanarayana. *J. Biol. Inorg. Chem.*, **18**, 751 (2013).
- [74] J.G. Liu, B.H. Ye, H. Li, Q.X. Zhen, L.N. Ji, Y.H. Fu. *J. Inorg. Biochem.*, **76**, 265 (1999).
- [75] P.K. Yata, M. Shilpa, P. Nagababu, M.R. Reddy, L.R. Kotha, N.M. Gabra, S. Satyanarayana. *J. Fluoresc.*, **22**, 835 (2012).
- [76] H. Zhang, F. Yang, Q Wu, S.Y. Liao, P. Liu, W.J. Mei, L. Li, S.Y. Zhang, X.C. Wang. *Med. Chem.*, **6**, 137 (2016).
- [77] G.B. Jiang, W. Li, J. Wang, B.J. Han, G.J. Lin, Y.Y. Xie, H.L. Huang, Y.J. Liu. *Transition Met. Chem.*, **39**, 849 (2014).
- [78] H.L. Huang, Z.Z. Li, X.Z. Wang, Z.H. Liang, Y.J. Liu. *J. Coord. Chem.*, **65**, 3287 (2012).
- [79] A. Srishailam, N.M. Gabra, Y.P. Kumar, K.L. Reddy, C.S. Devi, D.A. Kumar, S.S. Singh, S. Satyanarayana. *J. Photochem. Photobiol. B: Biol.*, **141**, 47 (2014).
- [80] E. Yabaş, E. Bağda, E. Bağda. *Dyes Pigm.*, **120**, 220 (2015).
- [81] M. Tarui, M. Doi, T. Ishida, M. Inoue, S. Nakaïke, K. Kitamura. *Biochem. J.*, **304**, 271 (1994).